

## THE SHAKEDOWN OF CIRCULAR ARCHES FOR MOVABLE LOADS

CZESŁAW CICHONŃ (KRAKÓW)

The static approach is applied to method analysis of arches under movable loads. The shakedown load value can be computed if the distribution of residual stresses is known, and limits of passive processes are evaluated in discrete numbers of the cross-sections layers. Numerical examples show that the first load passing is decisive and that the range of admitted shakedown loads is limited by value obtained from the first and the second passings.

### 1. INTRODUCTION

In the paper, the problem of computations of a circular arch for movable loads is considered. Owing to the assumed elastic-plastic properties of the material, the problem is much more difficult than this of the calculation of influence lines and is connected with the problem of the plastic shakedown of the structure.

The assumed model of the body and the static indeterminacy of the system cause the state of self-stresses in the arch after a certain number of passings, which may be advantageous for the arch. Namely, the loading, determined then, such that no further passing causes the increment of the permanent displacement, will be greater (or, at least equal), than the loading of the previous passings. We call it a shakedown loading for the arch after a definite number of passings. The proposed term stresses the essential features of the computed quantity, though it is not fully compatible with the definition within the classical theory of shakedown. Furthermore, it is shorter than the precise definition (the maximum value of the movable load, obtained after a definite number of passings, for which there is no increment of the permanent displacement of the arch in further passings).

In this paper, we deal with the problem of computations of the load, defined in this way.

To obtain the effective solution, the whole history of the loading process of the arch should be taken into account. This feature differs essentially (and makes more complicated) our problem from the classical problem of the shakedown of the structure.

The method of analysis, applied in the paper, is connected with B. G. NEAL's theorem [8], this being the particular case of MELAN's theorem [7] for the material with hardening.

A very few papers, concerning the analysis of elastic-plastic structures with movable loads, are available. These papers, e.g. [3, 5], are confined to the analysis of two- and three-span continuous beams, taking into account the bending moments

and considering ideal elastic-plastic properties of the material. The hardening of the material and the influence of the geometric non-linearities are taken into account in [4] for the analysis of the frame structure.

In the paper, the following basic assumptions are made.

1. The load consists of concentrated forces of the fixed direction and values independent of time, acting in the plane of arch, which is the principal plane of bending as well.
2. The change of position of the load on the arch is sufficiently slow to neglect the influence of the inertial forces and kinetic energy.
3. The principles of slender rods with small curvature are fulfilled (the considerations are limited to the axis of the arch and Bernoulli's principle of plain cross-sections works).
4. The influence of shear stresses on the deflection and yielding of the arch is disregarded.
5. The material, treated as the material continuum, is initially isotropic, elastic-plastic with the single linear hardening.
6. The structure of the material does not change during the process of loading.
7. Geometric equations are formulated for two cases:
  - i) under the assumption of geometric linearity, and
  - ii) with geometric non-linearity.

Below we list the main symbols used in the paper.

$a = A/E$	unitless coefficient in the physical equation,
$\alpha$	modulus of the material hardening,
$\beta$	angle of rotation of the normal vector to the axis of the rod,
$\zeta_k$	angle of disposition of the force $P_k$ on the arch,
$\varepsilon$	deformation,
$\varepsilon_p$	deformation on the yield limit,
$\varepsilon^p$	plastic deformation,
$e = \varepsilon/\varepsilon_p$	reduced deformation,
$e_g = \varepsilon_g/\varepsilon_p$	deformation on the boundary of the passive process,
$\vartheta = \varepsilon_0/\varepsilon_p$	deformation of the axis of the rod,
$e^* = \varepsilon^p/\varepsilon_p, s^* = \sigma^*/\sigma_p$	follower parameters in the physical equation,
$S^- = \sigma^-/\sigma_p, S^+ = S^*$	actual unitless yield limits for the compression and extension,
$S = \sigma/\sigma_p$	unitless stress,
$\sigma$	stress,
$\sigma_p$	yield limit,
$\varphi$	slope of the rod before deformation (independent variable),
$2F = 2(H_1 + H_2)B(z)$	area of the cross-section,
$\gamma_1 = 2H/R$	slenderness of the arch of the rectangular cross-section ( $H_1 = H_2 = H$ ),
$\gamma_2 = \frac{2F(H_1 + H_2)}{S}$	shape coefficient of the cross-section ( $S$ — elastic section modulus of cross-section),
$i$	cross-section number of the arch, $i = 0, 1, 2, \dots, J$ ,
$j$	position number of the load, $j = 0, 1, 2, \dots, J$ ,
$k = 2KH/\varepsilon_p$	unitless parameter of curvature,
$\lambda$	parameter of geometric non-linearity,

- $m = M/2FH\sigma_p$  unitless bending moment,  
 $n = N/2F\sigma_p$  unitless normal force,  
 $(n)$  number of passings of the load on the arch,  $n = 1, 2, 3, \dots, N$ ,  
 $p = P/2F\sigma_p$  unitless load,  
 $p_{SH}$  parameter of the shakedown load,  
 $r$  layer number for the sandwich cross-section,  $r = 0, 1, 2, \dots, R$ ,  
 $\rho = \sigma^r/\sigma_p$  residual unitless stress,  
 $t = T/2F\sigma_p$  unitless shear force,  
 $u = U/2H$ ,  $w = W/2H$  unitless tangential and normal displacements of the axis of undeformed arch,  
 $\psi$  angle coordinate of the point of the load disposition,  
 $Z$  loading program,  
 $2\theta$  central angle of the circular arch.

The asterisk\* denotes the quantities, memorised by the computer during the computations.

## 2. SHAKEDOWN LOAD FOR THE ARCH AFTER THE DEFINITE NUMBER OF PASSINGS

Let us assume that the load of the system agrees with the program of loading. We write this program in the form

$$(2.1) \quad Z = \{ \{P_k\}, \{\zeta_k\}, \{x_k\}, \{\psi_0^{(n)}, \psi_L^{(n)}\} \}, \quad k = 1, 2, 3, \dots, K.$$

In the above formula  $\{P_k\}$  is the set  $K$  of values of the system of loading forces,  $\{\zeta_k\}$  — the set of values of angles, determining the disposition of forces on the structure, and  $\{x_k\}$  — the set of numbers, determining the time independent configuration of loading. The method of passing of the load on the arch is established by the extreme positions  $\psi_0^{(n)}$  and  $\psi_L^{(n)}$  of the force, distinguished from the system of loading forces, as shown in Fig. 1.

For the cross-section with one axis of symmetry, the formula for stresses in the cross-section layer  $z = Z/(H_1 + H_2)$  takes the following unitless form

$$(2.2) \quad s^e(z) = n^e + \gamma_2 m^e z.$$

The index  $e$  in this formula indicates the elastic solution of the structure.

We write the yield condition for the cross-section in the form of the double inequality

$$(2.3) \quad s^-(z, t) \leq s^e(z) + \rho(z) \leq s^+(z, t).$$

In this formula,  $s^-$  and  $s^+$  are instantaneous (at the instant of time  $t$ ) limits of passive processes,  $\rho$  is the residual stress in the structure, resulting from the plastic deformation.

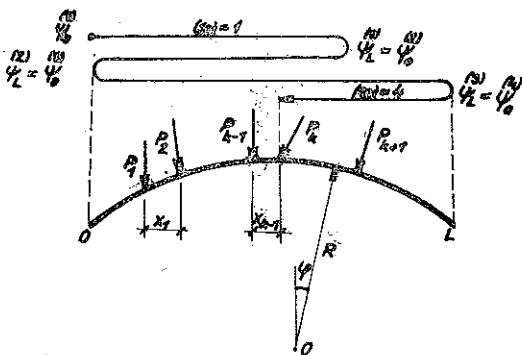


Fig. 1.

Further, we are dealing with the one-parameter load of the form

$$(2.4) \quad P_k = p P_k^0.$$

Then we can write for the elastic range

$$(2.5) \quad \begin{aligned} m^e &= p \bar{m}(\{p_k^0\}, \{\zeta_k\}, \psi, \varphi), \\ n^e &= p \bar{n}(\{p_k^0\}, \{\zeta_k\}, \psi, \varphi). \end{aligned}$$

We limit our considerations to countable sets  $i$  of cross-sections and  $r$  cross-section layers. Substituting (2.5) into (2.2), and subsequently into (2.3), we obtain the system of inequalities limiting the sought — for value of the load parameter of the  $r$ -th layer

$$(2.6) \quad \frac{s_r^- - p_r}{\bar{n}_i + \gamma_2 \bar{m}_i z_r} \leq p_r \leq \frac{s_r^+ - p_r}{\bar{n}_i + \gamma_2 \bar{m}_i z_r}.$$

Assuming that the conditions (2.6) hold for the equality sign, the parameter of the shakedown load  $p_{SH}$  for the whole arch can be found from the formula

$$(2.7) \quad p_{SH} = \min_i \min_r p_r.$$

Then we can find the shakedown load for the arch, making use of the relation (2.4).

The method proposed requires a systematic search of chosen layers of every cross-section of the structure for the successive load dispositions. The system of inequalities (2.3) allocates the elastic range for the cross-section on the plane  $(n^e, m^e)$  [6]. From this point of view, the shakedown parameter is the maximum value of the loaded parameter  $p$ , obtained for the isotropically "extended" path of loading [determined by the Eqs. (2.5)]. This extension is made to reach the point, common with the straight line, bounding the actual elastic region of the cross-section [2].

To use effectively the condition (2.7), the actual limits of passive processes  $s^-$  and  $s^+$  and the field of residual stresses  $\rho(z, \varphi)$  must be known. The method of computation of these quantities is presented in the next Section of the paper.

### 3. METHOD OF COMPUTATION OF THE ELASTIC-PLASTIC ARCH

#### 3.1. Physical equations

Let us assume that the arch is made of the elastic-plastic material with the single linear hardening, and the non-ideal Bauschinger effect. The adopted schematization of the plot  $s(e)$  is shown on Fig. 2.

Let us write the physical equation in the accrual form

$$(3.1) \quad \Delta s = a \Delta e,$$

where  $a=1$  — for passive processes,  $a=\alpha$  — for active processes.

We take account of the Bauschinger effect, introducing the measure of the effect  $\chi$ . This quantity sets the straight line, being the set of all points with the equal distance from the actual limits of passive processes. For limit cases, we have  $\chi=\alpha$  — ideal Bauschinger effect,  $\chi=0$  — isotropic hardening of the material.

We obtain the value of stresses  $s^-$  from the formulae:

for  $\chi = \alpha$

$$s^- = \frac{1-\alpha}{\alpha} e^* - 1,$$

for  $\chi \neq \alpha$

$$(3.2) \quad s^- = \left( \frac{2\chi}{1-\chi} - \frac{\alpha}{1-\alpha} \right) e^* - 1 \text{ — homogeneous passive process,}$$

$$s^- = \frac{2\chi}{1-\chi} e^* - s^* \text{ — multiple passive process.}$$

It follows from the above formulae, that to find  $s$  in the general case of cyclic processes and nonideal Bauschinger effect, two independent parameters  $s^*$  and  $e^*$  must be known. These are: the maximum stress and the corresponding plastic deformation, respectively. These quantities, containing the history of the loading process, must be calculated and actualized during the analysis. We achieve this by the use of memory of the computer.

In the problem under consideration, the appearance of multiple processes (e.g. cyclic) should not be excluded. We describe them through the formulae (3.1) and (3.2). The formulae correcting the values of  $e^*$  and  $s^*$  and the procedure itself have been presented in [1].

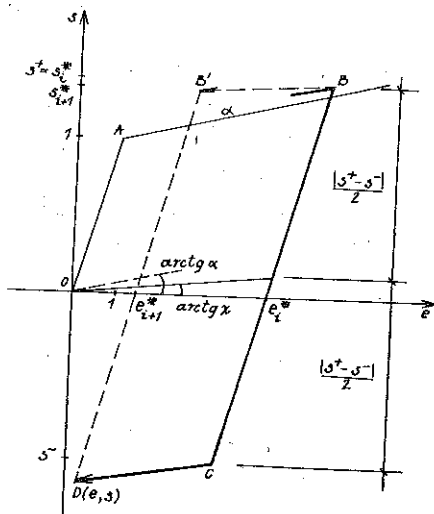


Fig. 2.

### 3.2. Governing equations for the arch in the accrual form

The system of governing equations for the elastic-plastic arches with movable load consists of six non-linear ordinary differential equations in their canonical form and two algebraic quasi-linear equations [1]:

$$(3.3) \quad \frac{du}{d\varphi} = \frac{\varepsilon_p}{\gamma_1} \ni -w - \lambda \frac{\gamma_1}{2} \left( \frac{dw}{d\varphi} \right)^2, \quad \frac{dw}{d\varphi} = u - \beta / \gamma_1,$$

$$\frac{d\beta}{d\varphi} = \frac{\varepsilon_p}{\gamma_1} k + \lambda \gamma_1 w, \quad \frac{dt}{d\varphi} = -n \left( 1 + \lambda \frac{d\beta}{d\varphi} \right),$$

$$\frac{dn}{d\varphi} = t \left( 1 + \lambda \frac{d\beta}{d\varphi} \right), \quad \frac{dm}{d\varphi} = -\frac{2}{\gamma_1} t (1 + \lambda \varepsilon_p),$$

$$(3.4) \quad \Delta n = I_0 \Delta \vartheta + \frac{1}{2} I_1 \Delta k, \quad \Delta m = I_1 \Delta \vartheta + \frac{1}{2} I_2 \Delta k,$$

$$(3.5) \quad I_l = \int_{-1/2}^{1/2} a(2z)^l dz, \quad l=0, 1, 2.$$

The discontinuities of the normal force  $n$  and the shear force  $t$  at the points of the load disposition should be taken into account in calculations.

$$(3.6) \quad \begin{aligned} n|_+ &= n|_- + p_k \sin(\theta - \psi_k - \lambda \beta_k), \\ m|_+ &= m|_- - p_k \cos(\theta - \psi_k - \lambda \beta_k). \end{aligned}$$

The parameter  $\lambda$ , introduced in the above equations, makes possible to include ( $\lambda=1$ ) or to neglect ( $\lambda=0$ ) the influence of geometric non-linearities (moderately large deflections) and the principle of stiffening on the deformation of the structure. The system of the Eqs. (3.3), (3.4) has been solved by the half-inverse method, presented in [1], changing the boundary problem into the problem with three initial conditions.

We express the increments from the Eq. (3.4) by the following formulae:

$$(3.7) \quad \begin{aligned} \Delta \vartheta &= \vartheta_{ij} - \vartheta_{ij-1}^*, & \Delta n &= n_{ij} - n_{ij-1}^*, \\ \Delta k &= k_{ij} - k_{ij-1}^*, & \Delta m &= m_{ij} - m_{ij-1}^*. \end{aligned}$$

The accrual method applied has eliminated, during the computation, the divergence of the iteration process resulting from the interaction of two discontinuities, namely the discontinuity of the derivative of the assumed extension plot and the discontinuities of the discretized cross-section, as shown in Fig. 3. The broken line stands for the plot of  $s(e)$ , where the loop may occur, as it actually is between points  $2'$  and  $2''$ .

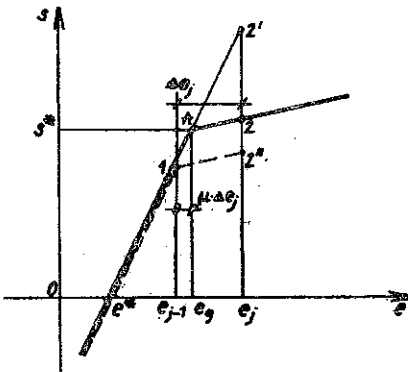


Fig. 3.

Below, we present the method of exact description of the plot  $s(e)$ . The idea of this method is to divide the increments  $\Delta \bar{n}$  and  $\Delta \bar{m}$ , corresponding to the transition of the state of stresses from the point 1 to the point 2 into parts  $\Delta \bar{n}$  and  $\Delta \bar{m}$ , for the point A of the plot to be admissible, and the remaining parts, necessary for the transition from the point A to the point 2. The point A is described by the corresponding deformation  $e_g$ .

The values of  $e_g$  versus the increments of the deformation  $\Delta e = e - e_i$  are laid down in the Table 1,  $e$  being the actual deformation, and  $e_i$  — actual value of plastic deformation.

Let  $\mu$  be the ratio of deformation increments

$$(3.8) \quad \mu = \frac{e_g - e_{j-1}}{\Delta e_j},$$

where

$$\Delta e_j = \Delta \vartheta + \Delta k \frac{r - 0.5 R}{R}.$$

Assuming the increments of the normal force and the bending moment to be sufficiently small, we can set

$$(3.9) \quad \Delta \tilde{n} = (1 - \mu) \Delta n, \quad \Delta \tilde{m} = (1 - \mu) \Delta m,$$

$$(3.10) \quad \vartheta_{j-1}^* := \vartheta_{j-1}^* + \mu \Delta \vartheta, \quad k_{j-1}^* := k_{j-1}^* + \mu \Delta k.$$

The values  $\Delta \tilde{n}$  and  $\Delta \tilde{m}$ , obtained from (3.9), we substitute into the system of equations (3.4), and then we find the increments  $\Delta \vartheta$  and  $\Delta k$ . Subsequently, according to (3.10), we calculate the deformation  $e_j$ . It corresponds to the transition from the point  $A$  of the plot to the point 2, the latter corresponding to the actual state of stresses.

Table 1.

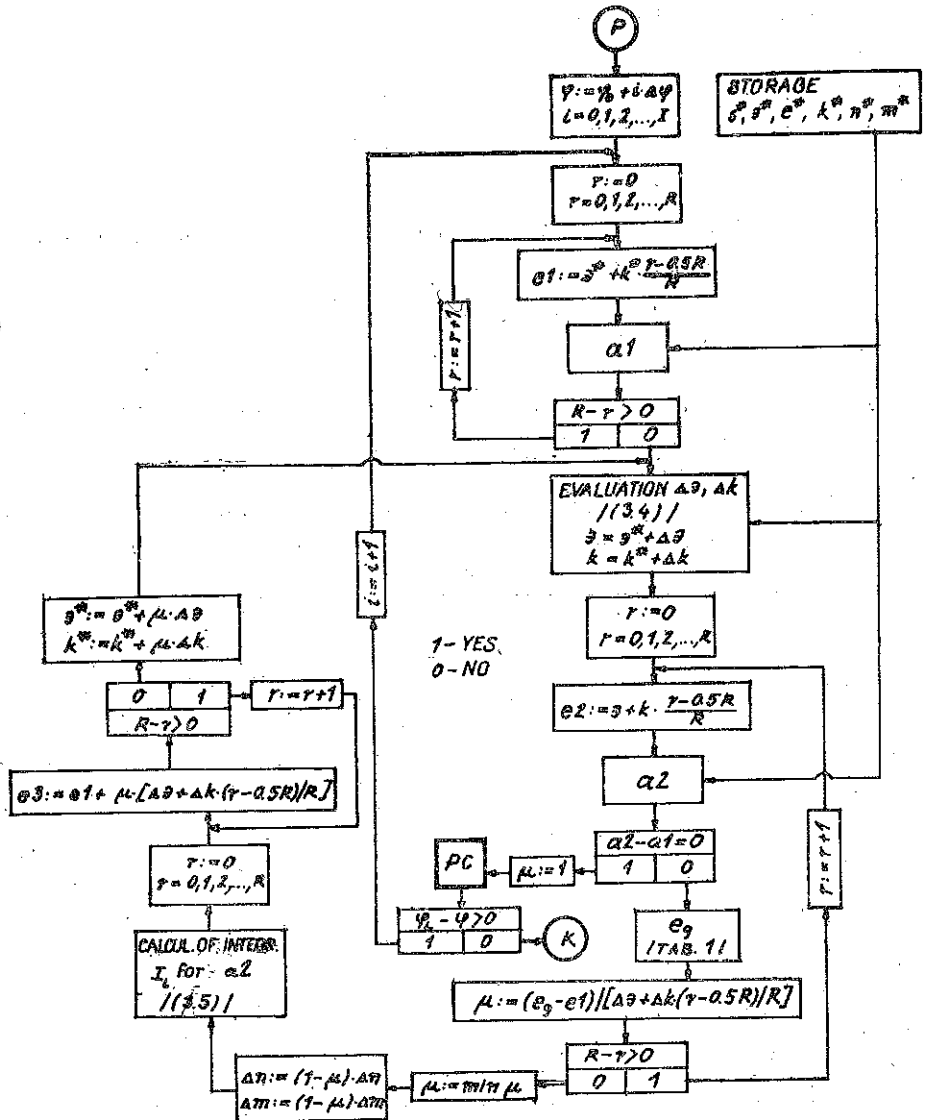
	$\Delta e = e - e_i$	$e_g$	
$\chi = \alpha$	$\Delta e > s^*$	$e^* + s^*$	
	$\Delta e < -s^* + \frac{2\chi}{1-\chi} e^*$	$\frac{1+\chi}{1-\chi} e^* - s^*$	
	$\Delta e > -s^* + \frac{2\chi}{1-\chi} e^*$	$\Delta e \geq 0$	$e^* + s^*$
		$\Delta e < 0$	$\frac{1+\chi}{1-\chi} e^* - s^*$
$\chi \neq \alpha$	$\Delta e > \frac{\alpha}{1-\alpha} e^* + 1$	$\frac{1}{1-\alpha} e^* + 1$	
	$\frac{\alpha}{1-\alpha} e^* - 1 \leq \Delta e \leq \frac{\alpha}{1-\alpha} e^* + 1$	$\Delta e \geq 0$	
		$\Delta e < 0$	
	$\Delta e < \frac{\alpha}{1-\alpha} e^* - 1$	$\frac{1}{1-\alpha} e^* - 1$	

If the situation described takes place in  $r$ -layers of the cross-section of the arch, the coefficient  $\mu$  is calculated as the minimum of all

$$(3.11) \quad \mu = \min_r \mu_r.$$

We finish this iteration process when the value  $\mu = 1.0$  is reached. The method is the particular case of the procedure applied in [9] for the material with multiple linear hardening.

The algorithm of the numerical integration of the set of the Eqs. (3.3) and (3.4) is presented in figure "Block diagram No. 1 — Numerical integration of the set of governing equations (3.3) and (3.4)". In the diagram,  $PC$  denotes the block of formulae of the adopted method of integration of the Eqs. (3.3).



Diag. 1.

The procedure presented can be used for the computation of elastic-plastic arches with an arbitrary disposition of loads. If the load were beyond the arch (the extreme force of the system of load placed on the support), then the resulting state of stresses would be the sought-for state of residual stresses. We compute the value of these stresses from the formula

$$(3.12) \quad p_r = e_r - e_r^*$$

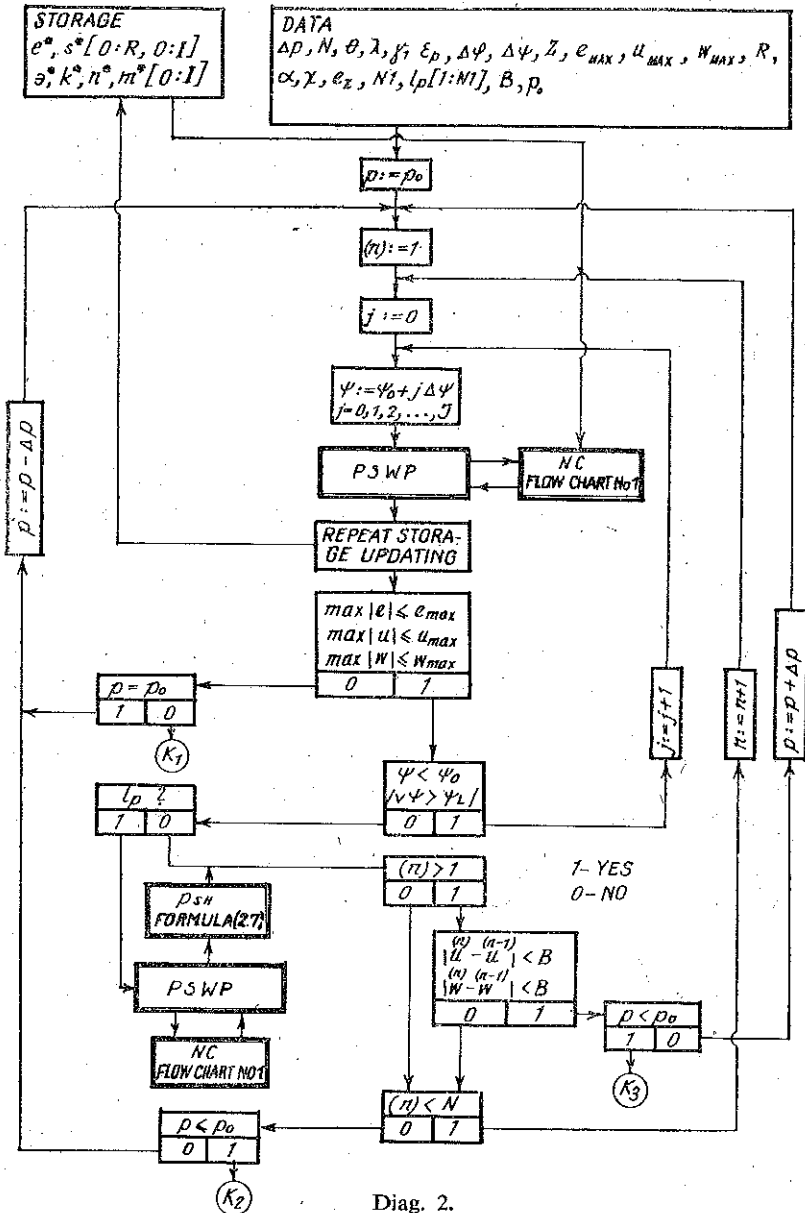
The elastic solution of the arch  $\bar{n}$  and  $\bar{m}$  follows from the repeated solution of the arch for  $p=1.0$ . We use here the set of the Eqs (3.3) und (3.6), in which  $p=1.0$ ,



$\lambda=0, \vartheta=n$  and  $k=m/6$  should be substituted. The set of the Eqs. (3.3) is then linear and the free initial conditions are found from the first approximation of the iteration process for the boundary conditions.

4. COMPUTATION ALGORITHM

The computation algorithm of elastic-plastic arches is presented in figure "Block diagram No. 2 — Computation of elastic-plastic arches for movable loads".



Diag. 2.

The program of computations consists of three main parts: the part containing the numerical integration — *NC* (the block diagram No. 1), the part of correction of the free initial values — *PSWP*, and the part containing the computation of the shakedown load —  $p_{SH}$  [the formula (2.7)]. The listed main parts of the program are connected to assure the automatic computation. We give the following input data: the support conditions of the arch — *SCH*, the value of the parameter  $\lambda$ , the loading program *Z*, the increment of the load  $\Delta p$ , the number of the load passing on the arch  $N$ , the number of switchings of the computation of  $p_{SH}$  —  $lp$  [ $1 : N_1$ ]. The algorithm makes possible to perform the calculations until either the given program of loading is realised, or the maximum value of the shakedown load is found, the latter for the case of the intervention of one of the following limitations: for the admissible displacement, or plastic deformation, or for the shakedown when  $(n) < N$ .

The ending of computations takes place in three different cases:  $K_1$  — excess of one of the limitations for  $u$ ,  $w$  or  $e$  under the load different from the initial  $p_0$ ;  $K_2$  — the shakedown did not happen either after the given number of passings, or for  $N=1$ ;  $K_3$  — the shakedown of the arch has taken place as the result of the decrease of load  $p_0$ .

The shakedown condition (non-increasing permanent displacements) is checked after every passing of the load on the arch.

## 5. NUMERICAL EXAMPLES

As an example, the simply supported circular arch of the rectangular cross-section  $2H \times 2B$ , loaded by the single vertical concentrated force, has been investigated (Fig. 4).

The boundary conditions for both supports of the arch are presented in the Table 2.

$X_1, X_2, X_3$  denote the free initial values. Introducing the parameter  $c$  into the formula for  $t$ , the boundary condition could be written for a particular position of the force, this being the point  $\varphi_0$ . If we assume  $\lambda=1$ , we obtain the two-point symmetric problem of the type "3+3" (three free initial values). On the other hand,  $\lambda=0$  is leading to the problem of the type "2+2" (two free initial values).

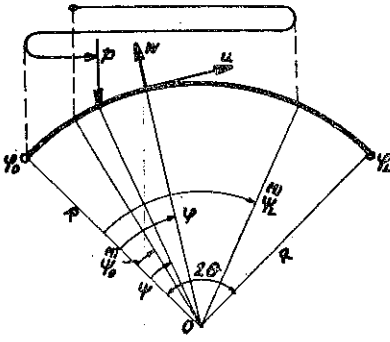


Fig. 4

The integrals (3.5) have been calculated, in particular cases, by the use of Simpson quadratic formula. Physically, this procedure means the replacement of the real cross-section by the substitutional sandwich cross-section with equidistant layers. The set of differential equations (3.3) has been integrated by the use of Runge-

Kutte formulae of the fourth order. The error has been estimated by the integration with a smaller step of integration, and the difference of results at the end-point  $\varphi_L$  has been used to measure the accuracy of calculations.

Basing on the presented block-diagram, the program in the language ALGOL-1204 has been prepared and the calculations have been carried out on EMC ODRA-1204.

Table 2.

Initial conditions ( $\varphi_0=0$ )	Final conditions ( $\varphi_L=2\theta$ )
$t=(1-\lambda) \left\{ n \operatorname{tg} \theta + \frac{p(1-c)}{\sin 2\theta} [\sin \theta + \sin (\theta-\psi)] \right\} + \lambda X_1$	$u=w=0$
$\beta=X_2, n=X_3, u=w=m=0$	$\lambda m=0$

$$c = \begin{cases} 1 & \text{for } \psi=0 \\ 0 & \text{for } \psi \neq 0 \end{cases}$$

The examples have been computed for the arch of the central angle  $2\theta=60^\circ$ , radius  $R=50$  cm and for the two- and five-layer cross-sections. The data of the material:

$$E=2.1 \times 10^6 \text{ kG/cm}^2, \quad \alpha=5 \times 10^{-3}.$$

### 5.1. Two-layer cross-section

The slenderness of the arch  $\gamma_1$  has been computed from the compatibility condition for surfaces and section moduli of the two-layer cross-section and for the optimal five-layer cross-section. We have assumed:  $\gamma_1=0.016$ ,  $\varepsilon_p=3.14 \times 10^{-4}$ ,  $\chi=\alpha$  (ideal Bauschinger effect),  $\Delta\varphi=2^\circ$ ,  $\Delta\psi=6^\circ$ ,  $B=1 \times 10^{-5}$ .

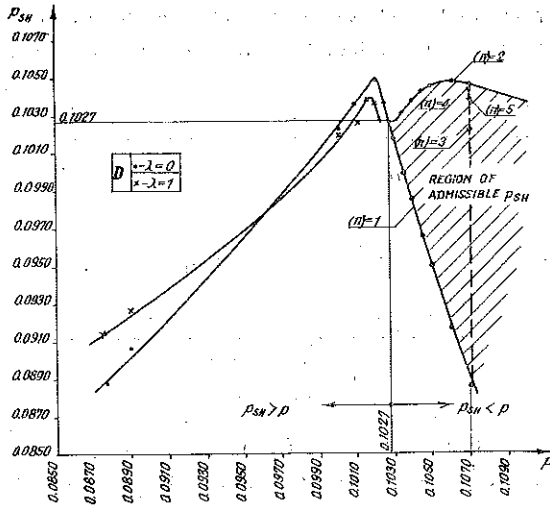
The computations have been carried out for three different loading programs

$$(5.1) \quad D1: \quad Z = \{ p, \theta - j\Delta\psi, j=1, 2, 3, \dots, J, 0, \{ \psi_0=2\theta - \psi_L^{(n)}, \psi_L^{(1)}=2\theta, \psi_L^{(2)}=0, \dots, \} (n)=1, 2, 3, \dots, N \},$$

$$(5.2) \quad D2: \quad Z = \{ p, \theta - j\Delta\psi, j=1, 2, 3, \dots, J, 0, \{ \psi_0=0^\circ, \psi_L^{(1)}=48^\circ, \psi_0^{(2)}=48^\circ, \psi_L^{(2)}=18^\circ, \psi_0^{(3)}=18^\circ, \psi_L^{(3)}=2\theta, \psi_0^{(n)}=2\theta - \psi_L^{(n)}, \psi_L^{(n)}=0^\circ, \psi_L^{(n)}=2\theta, \dots, \} (n)=4, 5, 6, \dots, N \},$$

$$(5.3) \quad D3: \quad Z = \{ p, \theta - j\Delta\psi, j=1, 2, 2, \dots, J, 0, \{ \psi_0=0^\circ, \psi_L^{(1)}=30^\circ, \psi_0^{(2)}=30^\circ, \psi_L^{(2)}=0^\circ, \psi_0^{(n)}=2\theta - \psi_L^{(n)}, \psi_L^{(n)}=2\theta, \psi_L^{(4)}=0^\circ, \dots, \} (n)=3, 4, 5, \dots, N \}.$$

The dependence of the shakedown load  $p_{SH}$  on the value of the load  $p$ , passing the arch according to the loading program D1, is shown in Fig. 5. For the load not exceeding the value  $p=0.1027$ , the shakedown of the arch has taken place after the first passing, and then  $p_{SH} > p$ . The biggest value of  $p_{SH}=0.1049$  has been obtained for  $p=0.1020$ . For the load  $p=0.1030$  and bigger, the shakedown of the arch has not occurred, and then  $p_{SH} < p$ . The striped region in the Figure contains the admissible values of  $p_{SH}$ ; it is limited by  $p$  on abscissa, for which the inadmissible deflections of the arch would appear.



$(n)$	$\rho$	$P_{SH}$	
		$\lambda=0$	$\lambda=1$
1	0.0875	0.0881	0.0915
1	0.0890	0.0900	0.0927
1	0.1000	0.1024	0.1019
1	0.1010	0.1036	0.1033
1	0.1020	0.1049	0.1036
1	0.1025	0.1035	
1		0.1019	
2	0.1030	0.1026	
1		0.1002	
2	0.1035	0.1032	
1		0.0985	
2	0.1040	0.1038	
1		0.0969	
2	0.1045	0.1043	
1		0.0952	
2	0.1050	0.1046	
1		0.0919	
2	0.1060	0.1048	
1		0.0886	
2		0.1046	
3	0.1070	0.1022	
4		0.1043	
5		0.1040	

Fig. 5.

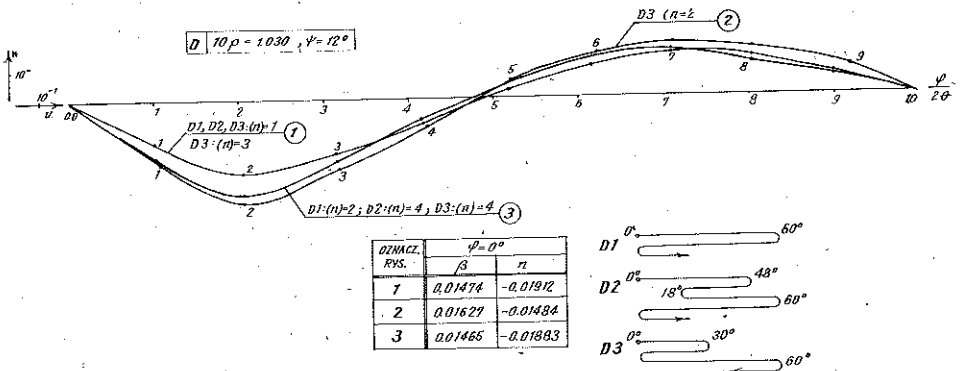


Fig. 6.

The programs *D2* and *D3* have been carried out for  $p=0.1030$  and  $\lambda=0$ . It follows from the computations that, after initial peculiar passings, the behaviour of the arch for further passings is similar to these for the program *D1*. The displacement line of the axis of the arch is shown in Fig. 6 for  $\psi=12^\circ$ . The plots for *D1*

Table 3.

<i>D</i>	<i>p</i>	$\lambda$	<i>(n)</i>			
			1	2	3	4
1	0.1030	0	0.1019	0.1026	0.1026	—
2			—	—	0.1026	—
3			—	0.1004	0.1019	0.1026

and  $(n)=2$ , *D2* and  $(n)=4$ , *D3* and  $(n)=4$  are the same. The values of  $p_{SH}$ , collected in the Table 3, confirm the feature of the structure to "forget" the past history of loading.

### 5.2. Five-layer cross-section

The slenderness of the arch has been assumed to be

$$\gamma_1=0.048, \quad \varepsilon_p=9.42 \times 10^{-4}, \quad \Delta\varphi=3^\circ, \quad \Delta\psi=3^\circ, \quad B=1 \times 10^{-5}.$$

The computations have been carried out for the program *D1*, for which we adopt the notation *P1* in the case of five-layer cross-section for  $\lambda=0$ , and *P2* — for  $\lambda=1$ . In the preliminary testing computations the yielding of different signs did not appear in the same layer of the cross-section. Therefore, the value  $\chi=\alpha$  has been taken, which is leading to the simplification of computations and, simultaneously, is the most disadvantageous case for the value of  $p_{SH}$ . The value of the passing load was  $p=0.125$ , the maximum number of passings  $N=5$ .

It follows from the performed computations that the utmost layers of the arch ( $r=0$  and  $r=4$ ) have been yielding in consequence of the action of the loads, the plastic zone for the layer  $r=4$  (external) being between the cross-sections  $6^\circ \leq \varphi \leq 54^\circ$ , and for the layer  $r=0$  (internal) — between the cross-sections  $9^\circ \leq \varphi \leq 18^\circ$  and  $42^\circ \leq \varphi \leq 54^\circ$ . The plastic zones have occurred during the first passing, and they have not increased during the next ones. Merely, the increment of the plastic zone has taken place in the layer  $r=4$  of the cross-section  $\varphi=48^\circ$ .

As an example, the stresses and deformations in the most strained cross-sections  $\varphi=12^\circ$  and  $\varphi=48^\circ$  are presented in the Tables 4 and 5.

The values of the shakedown load  $p_{SH}$ , computed for the successive passings of the load  $p=0.125$  are collected in the Table 6. Similarly to two-layer cross-section, the values  $p_{SH}$  converge to each other for even and odd passings, with the increasing number of passings.

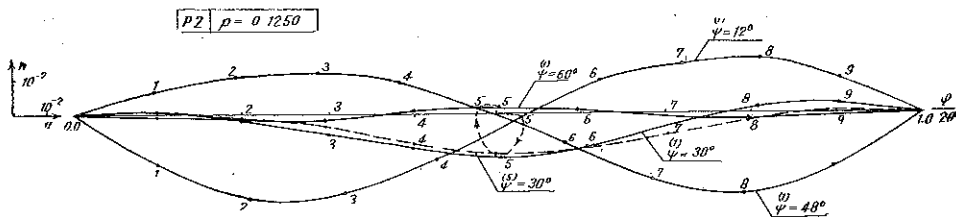
The displacement line for  $\lambda=1$  is presented in Fig. 7 for different positions of the force on the arch and different number of passings.

Table 4.

	$\varphi$	$r$		$(n)$				
				1	2	3	4	5
P1	12°	0	<i>e</i>	1.5339	1.4605	1.4295	1.4243	1.4243
			<i>s</i>	1.0027	1.0023	1.0021	0.9978	0.9978
		4	<i>e</i>	-1.7306	-1.6698	-1.6446	-1.6403	-1.6403
			<i>s</i>	-1.0037	-0.9424	-0.9175	-0.9132	-0.9132
	48°	0	<i>e</i>	1.3853	1.3802	1.4800	1.4880	1.4751
			<i>s</i>	1.0019	0.9969	1.0024	1.0024	1.0024
		4	<i>e</i>	-1.7048	-1.7007	-1.8112	-1.8114	-1.8281
			<i>s</i>	-1.0035	-0.9994	-1.0041	-1.0041	-1.0041

Table 5.

	$\varphi$	$r$		$(n)$				
				1	2	3	4	5
P2	12°	0	<i>e</i>	1.4812	1.3583	1.3583	1.3570	1.3570
			<i>s</i>	1.0024	1.0018	1.0018	1.0018	1.0018
		4	<i>e</i>	-1.7022	-1.6183	-1.6183	-1.6174	-1.6174
			<i>s</i>	-1.0035	-0.9146	-0.9146	-0.9137	-0.9137
	48°	0	<i>e</i>	1.3896	1.3851	1.4044	1.4043	1.4242
			<i>s</i>	1.0019	0.9974	1.0020	1.0020	1.0020
		4	<i>e</i>	-1.7123	-1.7086	-1.7394	-1.7394	-1.7704
			<i>s</i>	-1.0036	-0.9999	-1.0037	-1.0037	-1.0039



$(n)$	$\psi$	$\beta = 0^\circ$		
		$\beta$	$\alpha$	$t$
1	12°	0.00668	-0.14276	0.03504
	30°	-0.00072	-0.18942	-0.03733
	48°	-0.00310	-0.10599	-0.03402
	60°	0.00036	-0.00860	-0.00477
5	30°	-0.00056	-0.19282	-0.03938

Fig. 7.

Table 6.

	$p$	$\lambda$	$(n)$				
			1	2	3	4	5
$P$	0.1250	1	0.1078	0.1170	0.1102	0.1168	0.1103
		0	0.1113	0.1193	0.1144	0.1189	0.1147

## 6. CONCLUSION

The above-presented method of computation of elastic-plastic arches for movable loads and the computation of the shakedown load have proved to be effective and useful in applications.

The accrual form of the physical equation has advanced significantly the computations, in spite of the increment of the computer memory ( $e^*$ ,  $s^*$ ,  $\varepsilon^*$ ,  $k^*$ ,  $n^*$ ,  $m^*$ ).

The presented formulae and methods are simple in applications, and they work even in the case of the quasi-cyclic deformation processes with the mixed Bauschinger effect.

The loading program for the arch, described in the paper, admits the different ways of load passing to be considered.

In the case of foreseen significant deflections of the structure, the analysis can be carried out with the principle of stiffening neglected (i.e.  $\lambda=1$ ).

## 7. ACKNOWLEDGEMENT

The author wishes to express his gratitude to Prof. dr. Z. WASZCZYŹYŹYN for his valuable help during the formulation of the problem and working out the method of solution, as well as for the substantial current supervision of results obtained.

## REFERENCES

1. Cz. SICHON, *Metodyka obliczania przystosowania łuków sprężysto-plastycznych do obciążeń ruchomych*, Praca doktorska, Politechnika Krakowska, 1974.
2. Cz. SICHON, Z. WASZCZYŹYŹYN, *The shakedown of an elastic-plastic arch under movable load*, J. Struct. Mech., 3, 3, 1975.
3. Г. Д. Чернов, *Исследование приспособляемости неразрезных далок при подвижных нагрузках*, Изв. Выш. Техн. Учеб. Зав. Строит. и Арх., 6/1970, 23—29.
4. J. M. DAVIES, *The response of plane frameworks to static and variable repeated loading in the elastic-plastic range*, The Struct. Engin., 44, 8, 277—283, 1966.
5. Eyre G. DAYLE, *Shakedown of continuous bridges*, thesis presented to Washington University in partial fulfilment of the requirements for the Degree of Doctor of Science, June, 1969.
6. J. A. KÖNIG, *Theory of shakedown of elastic-plastic structures*, Arch. Mech. Stos., 18, 227—238, 1966.
7. E. MELAN, *Der Spannungszustand eines Hencky-Miseschen Kontinuums bei veränderlicher Belastung*, Sitz. Ber. Ak. Wiss. Wien, IIa, 147, 73—87, 1938.

8. B. G. NEAL, *Plastic collapse and shakedown theorems for structures of strainhardening material*, J. Aero, Sci., 17, 297-306, 1950.
9. W. WASZCZYŹYŃ, Cz. CICHON, Z. KĘPKA, *Symetryczna forma utraty stateczności sprężysto-plastycznego łuku kołowego*, Praca w przygotowaniu do druku.

## STRESZCZENIE

## PRZYSTOSOWANIE ŁUKÓW KOŁOWYCH DO RUCHOMYCH OBCIĄŻEŃ

Do analizy łuków poddanych ruchomym obciążeniom zastosowano podejście statyczne. Wartość obciążenia przystosowania obliczono na podstawie znanego rozkładu naprężeń resztkowych i granic procesów pasywnych w skończonej ilości warstw przekroju poprzecznego łuku. Przykłady numeryczne wykazują, że przejście pierwszego obciążenia jest decydujące, a zakres dopuszczalnych obciążeń przystosowania jest ograniczony przez wartości otrzymane z pierwszego i drugiego przejścia.

## Резюме

## ПРИСПОСОБЛЯЕМОСТЬ КРУГОВЫХ АРОК К ПОДВИЖНЫМ НАГРУЗКАМ

В настоящей работе для анализа арок подвергнутых действию подвижных нагрузок использован статический подход. Нагрузка приспособяемости вычисляется на основе найденных остаточных напряжений и пределов пассивных процессов в конечном числе слоев поперечного сечения арки. Из численного анализа следует, что решающим является первый переезд и что пространство допускаемых значений нагрузки приспособяемости ограничено значениями для первого и второго переездов.

TECHNICAL UNIVERSITY OF KRAKÓW

Received January 25, 1975.